Particle Accelerators, Vol. 59, pp. 19–41
Reprints available directly from the publisher
Photocopying permitted by license only

POSITRON SOURCES USING CHANNELING: A COMPARISON WITH CONVENTIONAL TARGETS

X. ARTRU[a], M. CHEVALLIER[a], V.N. BAIER[b], M.S. DUBROVIN[b], R. CHEHAB[c,*], A. JEJCIC and J. SILVA[d]

[a]*Institut de Physique Nucléaire, IN2P3-CNRS, 69622 Villeurbanne Cedex, France;* [b]*Budker INP, Novosibirsk 630090, Russia;* [c]*Laboratoire de l'Accélérateur linéaire, IN2P3-CNRS et Université de Paris-Sud, 91405 Orsay Cedex, France;* [d]*Collège de France, IN2P3-CNRS, Laboratoire de Physique Corpusculaire, 75231 Paris Cedex 05, France*

(Received 4 June 1997; In final form 29 September 1997)

A tentative comparison between positron sources using crystal or amorphous targets is presented. Both kinds of sources, dedicated to linear colliders, make use of multi-GeV incident electron beams. Considering a rather thick tungsten crystal (8 mm), such a target is placed in the usual working conditions of a linear collider, as the Japan Linear Collider (JLC) source, to which it is compared. Choosing a typical scheme for the positron accelerator, yields, energy deposited and heating of both targets are examined. Particular attention is put on the effects of the temperature on the crystal characteristics and performances. As the ability of a crystal positron source to sustain high intensities has to be checked, a test of radiation damage has been operated at SLC, which results are very promising. From this comparison, it appears that a tungsten crystal target, 8 mm thick, using channeling of 10 GeV electrons along its ⟨111⟩ axis provides almost the same yield at the Interaction Point of a linear collider as the classical source foreseen for JLC. Moreover, the energy deposited is about six times lower. At least, an hybrid solution made of crystal and amorphous disks of equal thickness is recommended. Its advantage is to preserve mainly the performances of the crystal in a warm regime.

Keywords: Channeling radiation; Pair creation; Positron source; Linear collider; Thermic effects; Warm crystal

* Corresponding author. Tel.: 033 1 64 46 84 77. Fax: 0033 1 69 07 94 04.
E-mail: chehab@lalcls.in2P3.fr.

1 INTRODUCTION

The enhancement of radiation observed for channeling conditions in a crystal, with respect to bremsstrahlung, makes such targets interesting for large positron yields: the high rate of photons generated along an axis produces a correspondingly high positron yield in the same crystal target. For incident electron beams, in the range 1–10 GeV, improvement in positron yields is expected in crystals of sufficient thickness (some mm) with respect to amorphous targets of the same thickness.[1]

Apart from the fundamental aspects of a comparison between crystal and amorphous targets, it is of interest and also useful to focus this comparison on "realistic" crystal/amorphous targets both dedicated to linear collider applications. "Realistic" might mean able to deliver enough positrons at the interaction point. More precisely, limitations due to wakefields put the level of the yield at about 1 e^+/incident e^- at the interaction point.

The linear collider projects, JLC, NLC (Next Linear Collider) and CLIC (Compact Linear Collider), are considering amorphous positron sources with impinging electron beams in the range 2–10 GeV.[2]

A comparison of a "realistic" crystal source with an amorphous one must concern not only the ability to reach the required yield but also some important problems as the heating of the target due to large amounts of deposited energy, the constraints put on the incident beam quality (emittance, energy dispersion) and some peculiar conditions associated with the crystalline nature of the target. For the sake of comparison, we have chosen the JLC project as the reference for the amorphous source. The same values of the incident energy (10 GeV) for both sources make the comparisons easier.

An experimental verification of the yield and transverse emittance of a crystal positron source should give definite answers on the useable positron yield for a LC (Linear Collider). The description of the experiment, foreseen on the transfer-line T_9 of the CERN-PS has been given previously.[3]

2 COMPARISON BETWEEN CRYSTAL AND AMORPHOUS TARGETS

After a short comparison between crystal and amorphous targets of the same thickness, emphasis will be put on crystal targets yielding the

same level ($1e^+/e^-$) at the interaction point as with the amorphous targets chosen in the LC projects.

2.1 Yield

2.1.1 *Compared Yields of Crystal and Amorphous Targets of the Same Thickness*

Comparisons of crystal and amorphous targets, both 4 mm thick, subjected to a 10 GeV incident electron beam have been made.[4] The evaluation of the accepted yield in the transverse phase space, using the JLC matching system, showed an enhancement of 3.3 for the crystal with respect to the amorphous target. An extensive comparison of crystal and amorphous targets of Si, Ge and W subjected to electron beams having a maximum energy of 5 GeV have also been undertaken.[5]

2.1.2 *Comparison of Crystal and Amorphous Sources Giving a Yield of $\sim 1\, e^+/e^-$ at the Interaction Point*

(1) *A typical scheme for a positron facility* is shown on Figure 1. The yields are generally calculated at:

- the target (total yield),
- the end of the matching system AD (accepted yield in transverse phase space),

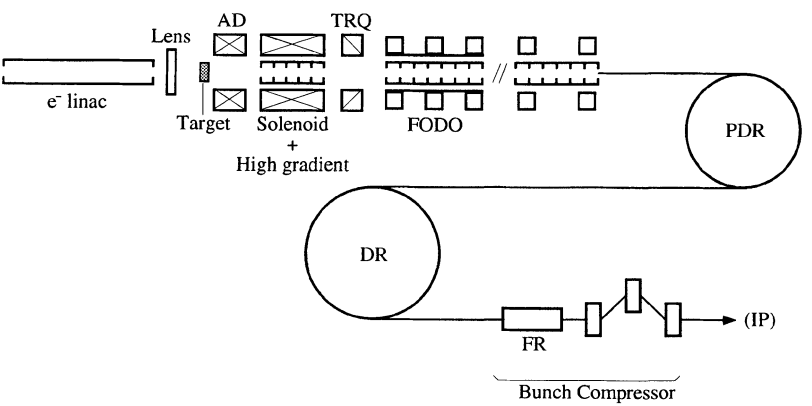

FIGURE 1 The positron facility, AD: adiabatic device; TRQ: matching optics.

- the entrance of the damping ring PDR (accepted yield both in transverse and longitudinal phase spaces),
- the interaction point.

(2) *The accepted yield in transverse phase space* depends strongly on the optical matching system chosen. Most of the projects have preferred the adiabatic lens studied first at SLAC.[6] Such a lens provides a rather good energy acceptance for the positrons and hence a relatively large yield.

As for the JLC project we shall adopt for our calculations the field law (see Figure 2):

$$B(z) = \frac{B_0}{1 + \alpha z} \tag{1}$$

with $B_0 = 8\,\mathrm{T}$, lens length $= 18\,\mathrm{cm}$, $\alpha = 50\,m^{-1}$.

(3) *Longitudinal phase space constraints.* As already pointed out [3] the spiralization of the positrons in the magnetic field of the matching system leads to a trajectory lengthening given by:

$$\delta L = \frac{\gamma_c \lambda_s}{4\epsilon} \theta_f^2 \ln \frac{\lambda_s}{\Lambda}, \tag{2}$$

where γ_c is the relative energy in the center of the accepted energy domain

$$\lambda_s = \frac{2m_0 c}{eB_s}, \qquad \Lambda = \frac{2m_0 c}{eB_0},$$
$$\epsilon = \frac{P}{eB^2} \frac{\mathrm{d}B}{\mathrm{d}z} \text{(parameter of smallness)}, \tag{3}$$

θ_f is the maximum angle at the end of the matching system. The expression above could be written more simply:

$$\delta L = \frac{\theta_i^2}{2\alpha} \ln \frac{B_0}{B_s}, \tag{4}$$

where θ_i is the maximum positron angle accepted by the matching system.

$$\theta_i = \sqrt{\frac{B_0}{B_s}} \theta_f. \tag{5}$$

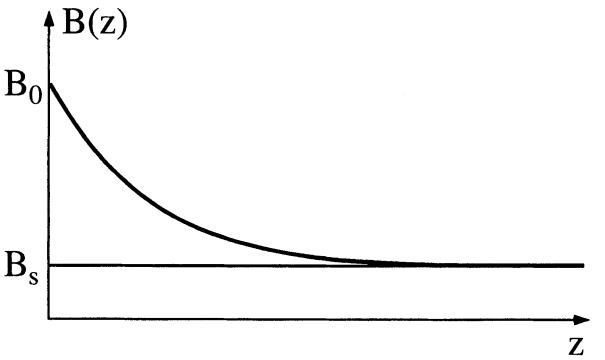

FIGURE 2 The "Adiabatic" magnetic field.

The limitation on the energy dispersion at the entrance of the damping ring (usually, $\delta E/E = \pm 1\%$) implies, correspondingly, a limitation on the bunch phase spread $\Delta\phi$, through the relation,

$$\frac{\delta E}{E} \sim \frac{1}{8}(\Delta\phi)^2 \tag{6}$$

and hence on δL. This latter limitation is introduced in GEANT and allows calculation of the accepted yield at the entrance of the damping ring. It is assumed that between the matching system and the damping ring no losses occur: such an hypothesis is reasonable and often considered.

2.1.3 *A Conventional Source Taken as a Reference: JLC*

In order to compare a crystal positron source to an amorphous one, we take as a reference the source proposed in the JLC project.[2] Such a source concerns a 10 GeV electron beam impinging on a $6X_0$ thick tungsten target. The yields indicated are:

- Total: 21 e^+/e^-
- Entrance of DR: 3.1 e^+/e^-
- Interaction point: 1.5 e^+/e^-

These yields have also been calculated, with GEANT code, using the matching device of JLC. The results agree with the data already published [2] and are represented on Figure 3 where the energy domain has

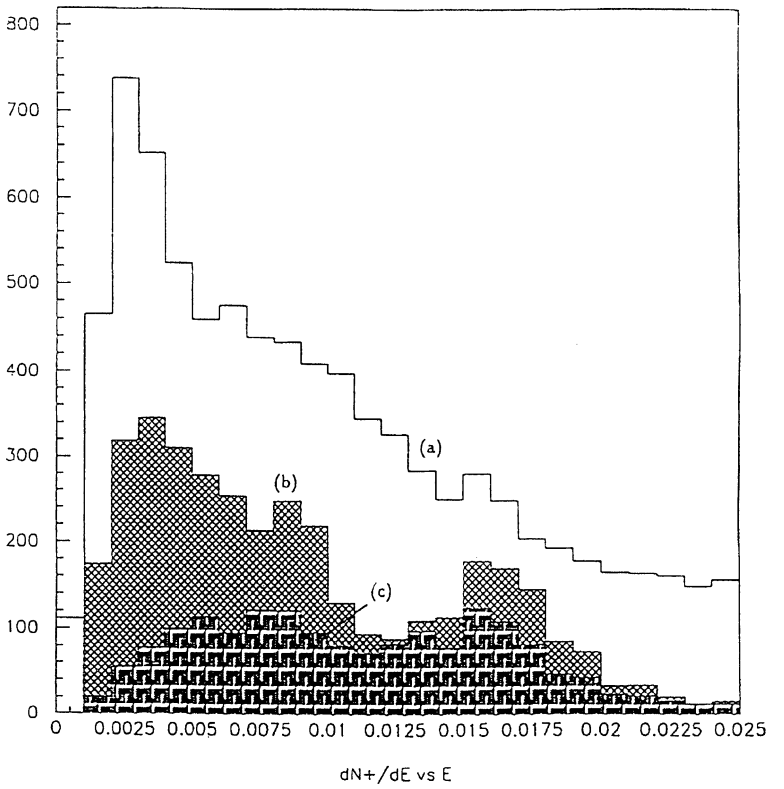

FIGURE 3 E^+ spectra for a $6X_0$ amorphous target: (a) total yield; (b) accepted yield in transverse phase space; (c) accepted yield in transverse and longitudinal phase spaces.

been restricted to the accepted one, with a superposition of three spectra: the total one, the accepted one in the focusing channel and the one accepted at the entrance of the damping ring. It is clearly seen on the pictures that, taking into account the longitudinal constraints associated with the energy dispersion at the entrance of the damping ring, the low energy part of the spectra is reduced. That corresponds to particles having long pathes of spiralization in the solenoïd and presenting, hence, large phase shifts with respect to the particle of reference.

If we take a transmission factor of 0.5, between the entrance of the damping ring and the interaction point as can be inferred from the observation of the tables in[2] the available yield at the IP is of 1.5 e^+/e^-.

Note: We can observe some kind of dip in the spectra around 10 MeV. This is related to the focusing conditions in the adiabatic lens. Varying the field value and the lens length we can move the dip location on the energy axis.

2.1.4 *A Crystal for a Positron Source*

Due to much shorter radiation lengths in crystals with respect to amorphous targets, a considerable amount of photons is emitted in the first millimeters of the crystal target. If we consider for instance a 10 GeV incident electron beam, most of the channeling radiation takes place in the 4–5 mm from the entrance face of the crystal. We can then consider that an 8 mm thick crystal give equivalent results for the positrons, when compared to an hybrid target made of a 4 mm thick crystal followed by a 4 mm amorphous tungsten target. Simulations with a dedicated code provided very close values of the positron yield for the two kinds of targets: slight differences might come from positron energy spectrum and emittance. Henceforth, we shall present the results of the simulations operated in the all-crystal solution.

Positron generation in an 8 mm tungsten crystal, axially oriented on its $\langle 111 \rangle$ axis, has been simulated using a dedicated code.[1] As in the case of an amorphous source, the yields have been evaluated at different locations. Their values are as follows:

- Total yield: $19\,e^+/e^-$
- Entrance of damping ring: $2.4\,e^+/e^-$
- Interaction point: $1.2\,e^+/e^-$

The results of the simulations are presented on Figure 4. Similar remarks, as for the amorphous target of JLC, can be formulated regarding the reduction of the low energy region of the spectrum. Concerning the yield at the interaction point, it reaches $1.2\,e^+/e^-$ with the same transmission factor between the DR and the interaction point as for the JLC.

The same remark can also be made concerning the dip in the energy spectrum, as for JLC.

We have represented on Figure 5 the correlations between energy and angle (a), longitudinal and transverse momentum (b), angle and transverse momentum (c), energy and transverse momentum (d) for the 8 mm thick crystal target.

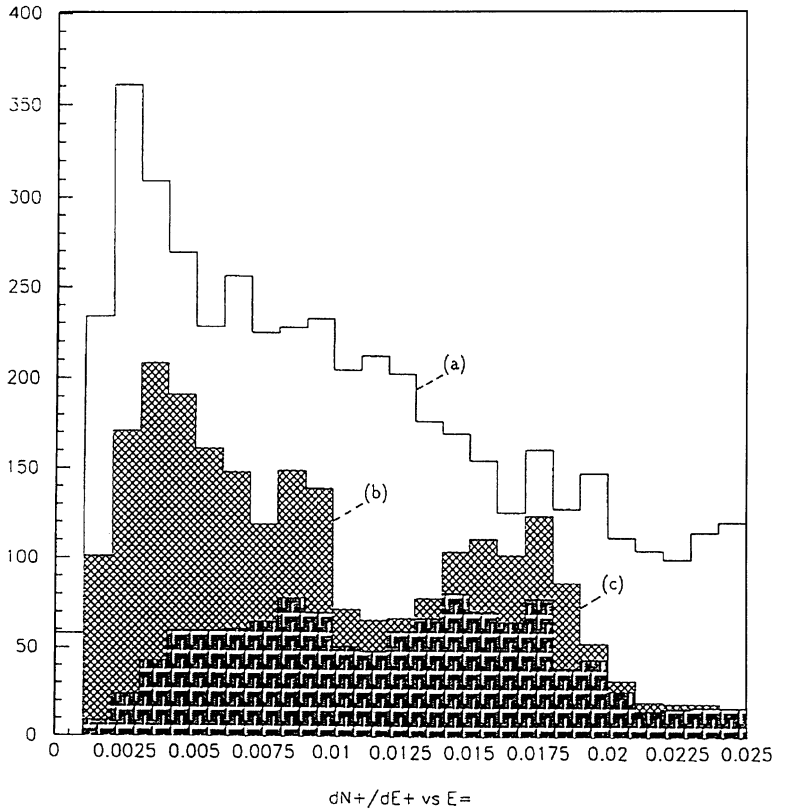

FIGURE 4 E^+ spectra for an 8 mm all-crystal: (a) total yield; (b) accepted yield in transverse phase space; (c) accepted yield in transverse and longitudinal phase space.

The angular restriction associated to the energy dispersion limitation at the entrance of the damping ring is represented by the line $\theta = 30°$ or $\theta = 45°$ for an S-band and an L-band positron accelerators, respectively. In order to give an illustration, a useful region has been hatched for one particular case $\theta = 30°$ and $p_\perp = 10\,\text{MeV}/c$ on Figure 5(b).

It can be seen that using an L-band positron accelerator, after the target, leads to a better acceptance than with an S-band one. This is due to the fact that the large radii ($\sim 20\,\text{mm}$) associated with the L-band structures allow transverse acceptance improvement and do not have drastic influence on the bunch lengthening because of the large radio-frequency wavelength value.

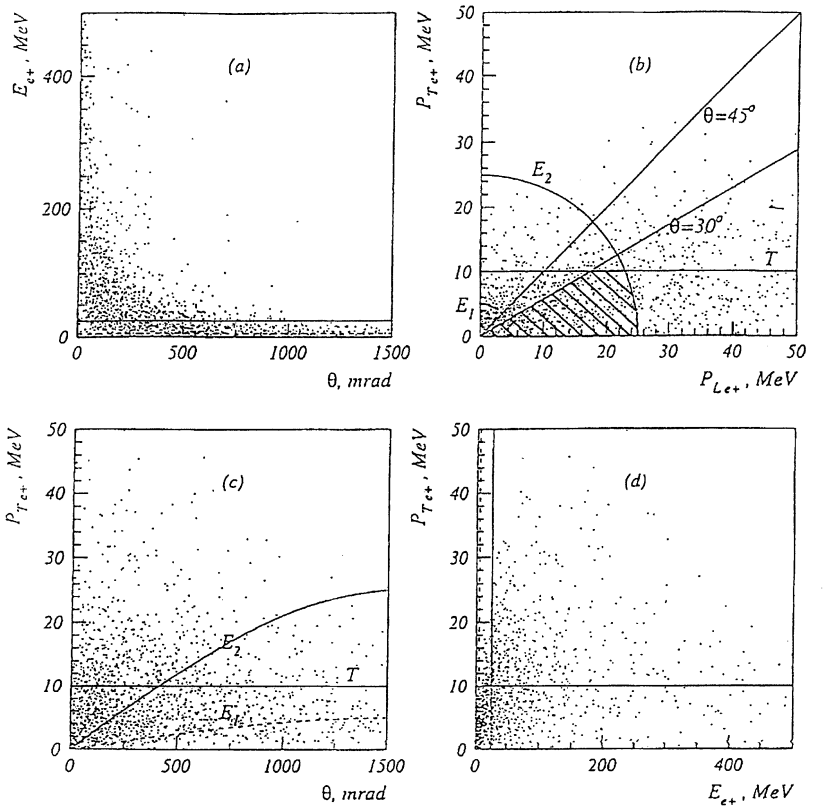

FIGURE 5 (a) Correlation between energy and angle; (b) longitudinal and transverse momentum; (c) angle and transverse momentum; (d) energy and transverse momentum for positrons from crystal target for 10 GeV incident electron energy. Lines and curves in the scatter plots show corresponding energy (E_1, E_2), transverse momentum (T) and angular (θ) borders.

2.2 Heating

A large amount of power is deposited by the shower in the target. Due to the volumetrically nonuniform power deposition, mechanical stresses may arise causing target failures. Such problem has been studied and systematic measurements operated at SLAC.[7] A limit on the incident electron energy density has been derived:

$$\rho = \frac{N^- \cdot E^-}{\pi\sigma^2} < 2 \times 10^{12}\,\mathrm{GeV/mm^2}, \tag{7}$$

where N^-, E^- and σ represent the number of incident electrons per linac pulse, the energy and rms beam radius, respectively. This limit is taken into account in the LC projects and so on for the crystal source.

2.2.1 *Energy Deposited in the Target*

The fraction of incident energy deposited in the target has been evaluated for the amorphous and crystal targets. We have represented this amount for the three linear collider sources (CLIC, NLC, JLC) using conventional targets, on Figure 6. The comparison is made with a crystal target (W;⟨111⟩) giving a similar yield ($\sim 1e^+/e^-$) at the interaction point, i.e. 8 mm thick. For a 10 GeV incident beam, this ratio is about 32% for the JLC source whereas it is of 5% for the crystal source.

As far as the qualities of the crystal depend on the local temperature the heating distribution in the crystal volume has to be carefully described.

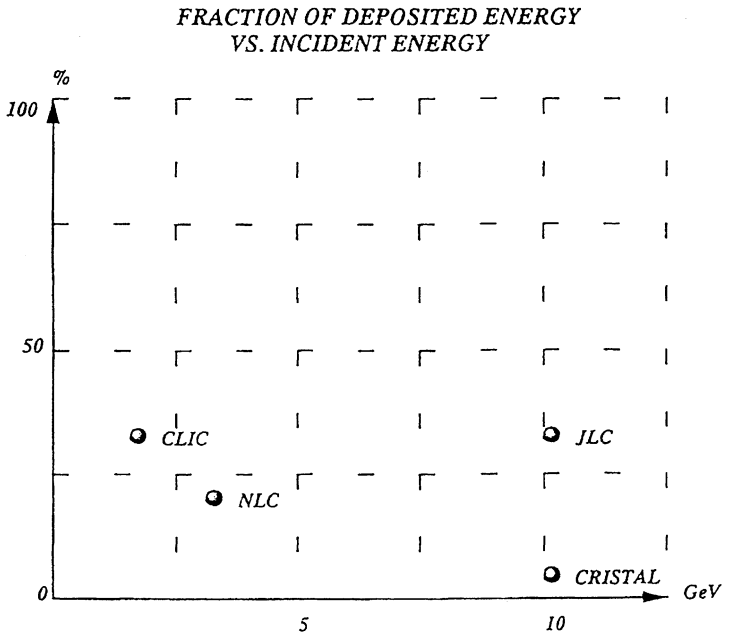

FIGURE 6 Energy deposited in the target.

Two simulations codes[8,9] using finite element methods, allowed exact determination of the temperature distribution inside the target. Both codes (SYSTUS and PROMETHEE) present good agreement on the results. We represent on Figure 7 the temperature distribution in the JLC amorphous target submitted to the nominal incident electron beam ($E = 10\,\text{GeV}$; $N = 5 \times 10^{11}\,e^-/\text{pulse}$). The average temperature reached in the case of the target leads to the choice of a rotating system to prevent material destruction.

Simulation in a fixed crystal target, 8 mm thick, submitted to the same incident beam as for the JLC shows local temperature at the exit face of the target of about thousand degrees Celsius. Such temperature

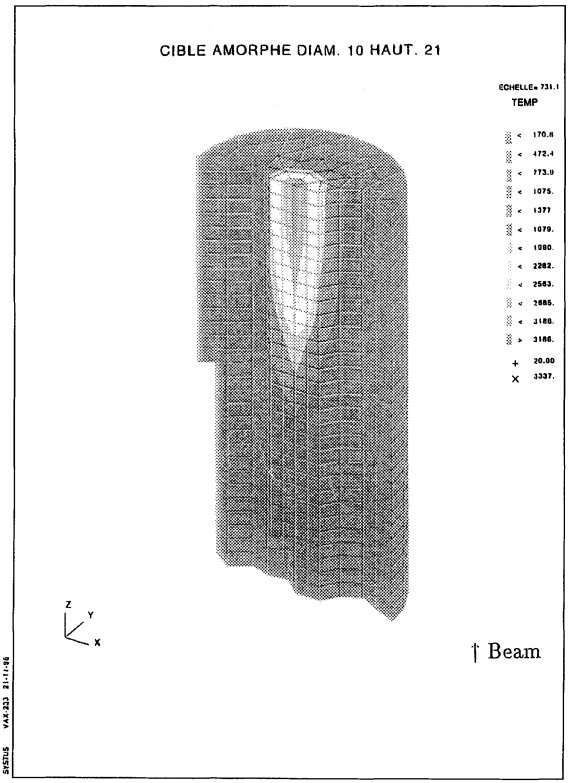

FIGURE 7 Simulation of the temperature distribution in the JLC e^+ source (SYSTUS code). Water cooling is ensured on the cylindrical target surface with a reference temperature of 20°C. (See color plate I.)

could affect the crystal characteristics. We consider, then, the hybrid solution with a 4 mm thick crystal followed by another 4 mm thick amorphous target. As photon generation takes place mainly in the crystal and pair creation in the amorphous target, the main part of the deposited energy is in the amorphous part of the positron source; therefore, heating in the crystal does not exceed reasonable values. We represent on Figure 8 the temperature distribution in the two parts of the target as simulated with the PROMETHEE code.[9]

It can be seen that the temperature, at the exit face of the crystal, does not reach 500°C; the temperature at the exit face of the amorphous element exceeds 2000°C. The same solution for this amorphous part, as for JLC, could be applied putting these amorphous targets on a rotating wheel to prevent high average temperatures.

2.2.2 *The Crystal in Warm Regime*

Heating the crystal, with the energy deposited by the shower, makes the thermal vibration amplitude u_1 larger. As the radiation intensity spectrum, in channeling conditions, is a decreasing function of u_1,[5] this intensity becomes lower when the crystal is heated.

We can observe the effects of the temperature on the continuum potentials of the $\langle 111 \rangle$ axis (Figure 9). These potentials have been estimated using the expression given by Baier *et al.*[10]

$$U(x) = V_0 \left[\ln\left(1 + \frac{1}{x+b}\right) - \ln\left(1 + \frac{1}{x_0+b}\right) \right], \tag{8}$$

where

- $V_0 = Ze^2/d = 430$ V, for the tungsten crystal oriented along its $\langle 111 \rangle$ axis,
- $x = \rho^2/a_s^2$; ρ being the distance to the axis and a_s, the screening radius,
- $b = 2u_1^2/a_s^2$; u_1 being the thermal vibration amplitude,
- $x_0 = S/\pi a_s^2$; S being the entire area associated with individual axis,
- u_1 is increasing with the temperature; its values is derived from Gemmel[11] and given in Table I.

It can be seen that the potential, on the axis, is decreasing by a factor 2 when the temperature grows from the normal level to ~ 930°C. One

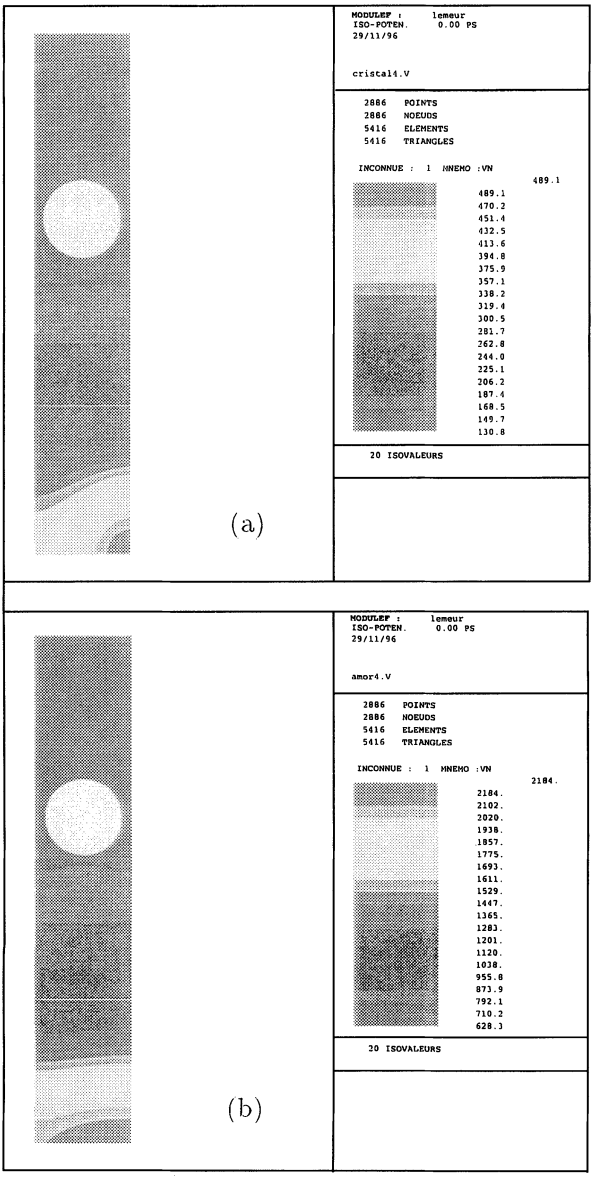

FIGURE 8 Simulation of the temperature distribution in the hybrid source (PROMETHEE code). 2D radial view of the two elements of the hybrid source. (a) The 4 mm crystal; (b) the 4 mm amorphous disk, placed downstream of (a); water cooling is represented by the white circle. (See color plate II.)

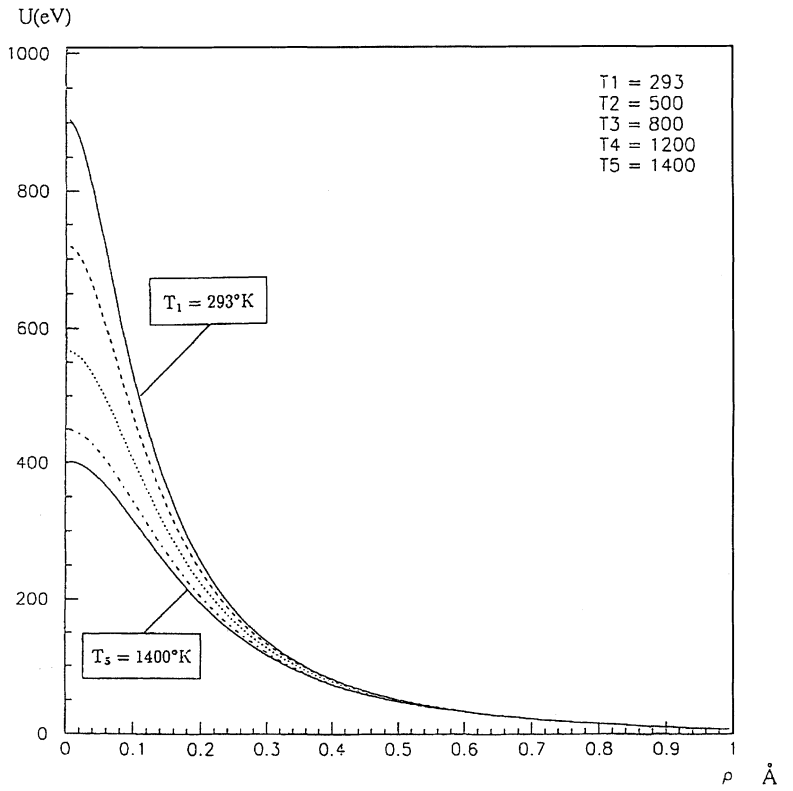

FIGURE 9 Continuum potentials for the ⟨111⟩ axis of the tungsten crystal. The temperatures are expressed in K.

TABLE I Thermal vibration amplitude (u_1)

T (K)	400	500	600	700	800	1000	1200	1400
UTHERM (u_1)	0.058	0.065	0.071	0.077	0.082	0.091	0.100	0.109

of the consequences is the restriction on the critical angle. For the case considered above and for 10 GeV it changes from 0.45 to 0.32 mrad.

2.2.3 *Effects of the Temperature on the Positron Yield*

Some simulations have been undertaken varying the temperature in the crystal and observing the photon and positron yields. The latter has

been considered at two locations:

- at the exit of the target (total yield),
- at the entrance of the damping ring (accepted yield in transverse and longitudinal phase spaces).

The acceptance conditions are the following:

$$\begin{aligned} &5 \leq E^{+} \leq 25\,\text{MeV}, \qquad p_{\perp} \leq 8.4\,\text{MeV/c}, \\ &r \leq 0.35\,\text{cm}, \quad \text{at the source} \end{aligned} \tag{9}$$

and $\delta L \simeq 1.19\,\text{cm}$ (limit on longitudinal acceptance) at the end of the adiabatic device. The results can be summarized as follows:

For the photons

Simulations made in a 4 mm thick tungsten crystal showed that the yield is decreasing by an amount of $\sim 20\%$ when the temperature grows from the ambient to $\sim 600°\text{C}$.

For the positrons

- For a 4 mm thick crystal, the decrease of the total positron yield is on the same level, as for the photons, when the temperature grows from the ambient to 600°C.
- For an 8 mm thick target, we considered two cases:
  - a whole crystal target,
  - an hybrid target with 4 mm crystal followed by a 4 mm amorphous disk.

The results are summarized on Table II on which we have also reported the corresponding data for the amorphous target for the sake of comparison. The yields of the amorphous converter are supposed unchanged with the temperature increase.
Some remarks could be added to this table:

- A normalisation to the intensity available at the interaction point for JLC [2] has been operated. This gives different values for the necessary incident electron beam on the crystal target. The value of $5 \times 10^{11}\ e^{-}$/pulse for the crystal target corresponds to that taken for the temperature distribution simulation (Figure 8).

TABLE II Compared characteristics for the 3 converters

	Total yield		*Accepted yield* $T=600°C$ *for crystal*	
	$T=20°C$	$T=600°C$	*at DR*	*at IP*
8 mm W crystal	19.1	16.3	2.	1.
4 mm W crystal + 4 mm amorphous	18.3	16.5	2.1	1.05
21 mm amorphous	21	21	3.1	1.55
	e^-*beam for* 5×10^{11}*at IP*	*Beam power* kW	*Target power* kW	*Target peak temperature* (°C)
8 mm W crystal	5×10^{11}	120	6.6	1400
4 mm W crystal + 4 mm amorphous	5×10^{11}	120	6.7	2184*
21 mm amorphous	3.3×10^{11}	79	27	2102

*in amorphous disk

- The difference between the energies deposited in the target for the all-crystal and hybrid target is mainly due to the slight difference in the number of secondary particles of the shower.
- Concerning the peak temperature in the target, we supposed that all the targets were fixed in position, which is, of course, an irrealistic statement for the amorphous converter. The difference in peak temperatures for the all crystal and hybrid targets may be explained by the fact that most of the energy is deposited in the second part of the converter and that in the hybrid case the corresponding cooling area is smaller than in the all crystal case.

The observations on the yield which could be inferred from this table are the following:

- the yield is lowered by an amount of 10% for the hybrid target and of 15–20% for the all crystal target when the temperature grows from the ambient to $\sim 600°C$;
- referring to the heating calculations (see Figure 8) the temperature increase associated with a 10 GeV beam of 5×10^{11} e^-/pulse and 150 Hz ($\sim 500°C$) is smaller than the 600°C considered in the table, henceforth the crystal performances of the hybrid solution might be better and so on for the yields.

The accepted spectra for the two temperatures considered, and for the all crystal case are shown on Figure 10. We recall that for JLC like

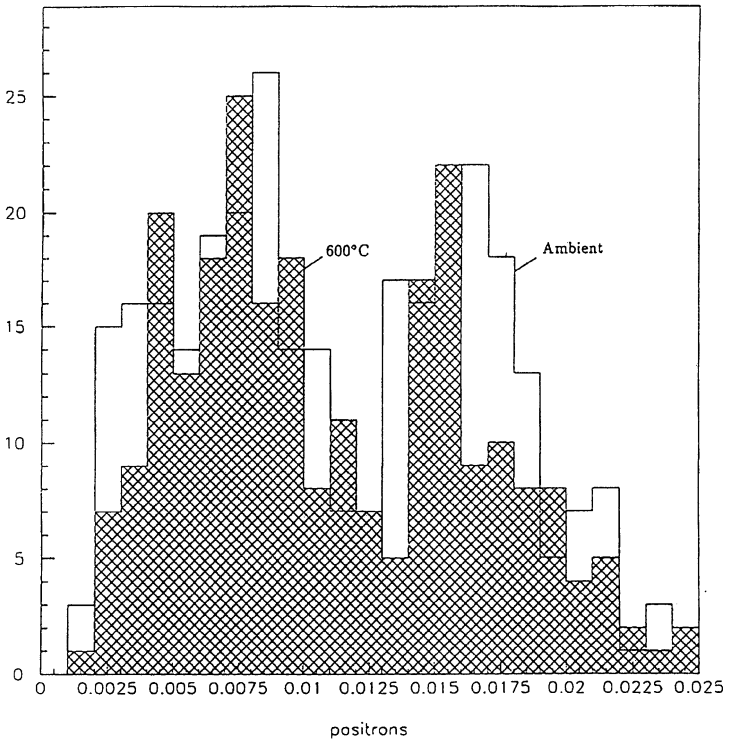

FIGURE 10 Positron energy spectra for an 8 mm all-crystal.

conditions and for the expected temperature increases, the hybrid solution is to be considered.

Pulse temperature rise and associated stress

The temperature rise from a single beam pulse corresponding to a small beam could be large enough to cause failures in the target material. That situation corresponds to a thermal shock. We shall, first, evaluate the temperature rise in both kinds of targets – amorphous and hybrid crystalline – and calculate, later, the maximum temperature rise which could be tolerated.

(a) *Pulse temperature rise*: The pulse temperature rise is given by:[12]

$$\Delta l_{\mathrm{p}} = \frac{NE_0}{\rho C_p}\left(\frac{1}{E_0}\frac{\Delta E}{\Delta v}\right) \tag{10}$$

where N is the number of particles per pulse, ρ the material density, C_p the heat capacity and $(1/E_0)(\Delta E/\Delta v)$ is the energy deposition rate per unit volume in the target with E_0 as the incident energy.

As most of the energy is deposited in the last fraction of the converter, we consider the deposition in the second half of the target.

For the amorphous target [JLC]

With $N = 3.3 \times 10^{11}\,e^-/\text{pulse}$, $\sigma = 3\,\text{mm}$,
target thickness $= 21\,\text{mm}$, deposited energy $= 138\,\text{J/pulse}$,
we get : $\Delta t_p = 180\,\text{degree/pulse}$.

For the crystal target [4 mm crystal + 4 mm amorphous]

With $N = 5 \cdot 10^{11} e^-/\text{pulse}$, $\sigma = 3\,\text{mm}$,
target thickness $= 8\,\text{mm}$, deposited energy $= 37\,\text{J/pulse}$,
we get : $\Delta t_p = 125\,\text{degree/pulse}$.

(b) *Mechanical stresses*: The mechanical stress induced by the thermic gradients inside the target material is given by

$$P_t = \alpha E \Delta T, \tag{11}$$

where α is the coefficient of linear expansion $[K^{-1}]$, E the elastic modulus (Young) $[N\,m^{-2}]$ and ΔT is the temperature gradient.

If we put a limit on the maximum stress P_{tm}, choosing for instance the value for which the material deformation ceases to be elastic, we can get for the maximum tolerable temperature rise:

$$\Delta T_m = P_{tm}/(\alpha E). \tag{12}$$

For W–Re,

$P_{tm} = 91 \cdot 10^7\,\text{Nm}^{-2}$, $\alpha = 5 \cdot 10^{-6}\,\text{K}^{-1}$, $E = 4 \cdot 10^{11}\,\text{Nm}^{-2}$,
we get $\Delta T_m = 450\,\text{K}$

If we consider pure tungsten, W, the corresponding value for the maximum temperature rise is about 270 degrees; the difference is due mainly to the P_{tm} value, which is twice smaller in the case of pure W.

These tolerable temperature gradient values are above the temperatures rises foreseen for the targets and due to pulse heating.

These estimations will be followed by a more exact calculation, using a finite element method which is under development in the PROMETHEE code.[9] The results will be published in a forthcoming report.

3 QUALITIES OF THE INCIDENT ELECTRON BEAM

As it is well known, the channeling condition is expressed through the inequality:

$$\psi < \psi_c = (2V_0/E_0)^{1/2}, \tag{13}$$

where ψ is the incident angle, ψ_c the critical angle [Lindhard], V_0 the depth of the potential well created by the atomic rows and E_0 the incident energy. This condition gives rise to additional operational constraints. For the $\langle 111 \rangle$ axis of tungsten, V_0 is about 940 eV at normal temperature; the critical angle at 10 GeV is of 0.45 mrad. It requires that:

- the mosaic spread should be less than 0.5 mrad,
- the electron beam emittance should be low enough to allow beam divergence values lower than 0.5 mrad.

Nevertheless, as crystal effects persist up to two to three times the critical angle ψ_c, the above condition appears somewhat restrictive.

3.1 Incident Beam Dimensions

As the crystal converter is thinner than the amorphous one leading to smaller positron source size it is reasonable to consider incident beam dimensions with larger values: σ^- could be closer to 2 mm for the incident beam.

A typical, though restrictive, phase-space for the incident beam emittance in each transverse phase plane x/y could be as represented on Figure 11.

The emittance area is

$$\epsilon_{x,y} \sim 0.5\pi \text{ mm mrad}. \tag{14}$$

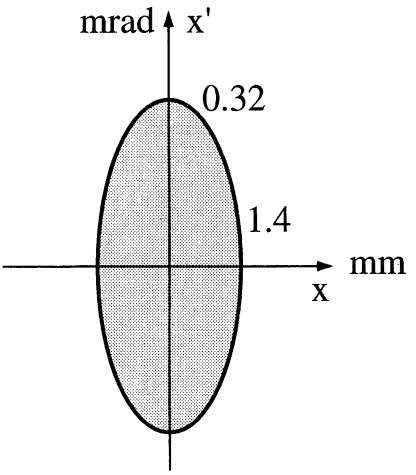

FIGURE 11 Typical emittance for the incident beam (10 GeV).

Such emittance is easily met at $E^- = 10\,\text{GeV}$ and even at significantly lower energies.

Requirements on $\delta p/p$

Due to chromatic effects on the incident beam transport by the quadrupole lenses, the beam spot at the converter entrance depends on the beam energy dispersion. An excessive energy dispersion could then lower the positron yield due to the geometrical acceptance limits of the positron accelerator. For a crystal converter, for which the tolerated beam dimensions could be larger, the limitations on the beam energy dispersion appear less severe.

4 CONSTRAINTS ASSOCIATED WITH AN INTENSE INCIDENT BEAM ON A CRYSTAL TARGET

A positron source is supposed to withstand very high power levels of the incident electron beam. Hence, reliability of crystal sources is based on their long-time resistance to radiation damage and their possibility to keep high values of crystalline fields even when heated by the energy deposited by the shower (see Section 2.2.2).

Radiation damage

The radiation damage in the crystal, caused mainly by Coulomb scattering of the electron beam on the nuclei, has been evaluated and experiments have been undertaken.[1,4] A test with the incident electron beam on the positron source of the SLAC Linear Collider has been done recently. The integral density on the crystal was of $2\times10^{18}\,e^-/mm^2$ [13] which represented an analogous rate as for BNL experiment.[14] The crystal has been under analysis at the Max-Planck Institute, in Stuttgart. The first analysis by γ-diffractometry did not show any measurable damage on the irradiated zone of the crystal. Full results will be published later.

5 SUMMARY AND CONCLUSIONS

- A comparative study of conventional and crystal positron sources using the same kind of incident electron beam showed that:
  - A similar yield ($\sim 1e^+/e^-$) at the interaction point could be reached with an 8 mm thick tungsten crystal oriented along its $\langle 111\rangle$ axis, as with a JLC-like amorphous target (21 mm thick). Adjustment of the final positron intensity, at the IP, so as to equalize exactly that of the JLC can be operated using a slightly higher incident intensity on the crystal with, correspondingly, a larger electron beam size: the electron energy density on the target could then be preserved.
    The comparison has been undertaken with the same matching system for both sources. Informations to be gathered in the projected crystal source test should allow the optimization of the matching device with respect to the characteristics of the positron beam.
  - The heating of the target due to the important fraction of energy deposited by the shower is an important problem for all sources. However, the crystal source presents a much lower rate deposition (5% instead of 32%) than the JLC taken as a reference. The increase of the incident beam intensity does not affect strongly the ratio of the deposited powers. Practical solutions as rotating targets have been considered and used (at SLAC) for amorphous sources. A corresponding solution for the crystal targets so as to

lower the amount of average power must be studied carefully: the orientation constraints need some special arrangements.

- A tungsten crystal, 4 mm thick, provides about half of the yield value expected with an 8 mm thick crystal; the deposited energy is, in that case, 1% of the incident energy. An association of a tungsten crystal 4 mm thick with an amorphous tungsten target of the same thickness, put downstream, provides about the same yield as for the 8 mm crystal, as confirmed by the simulations. This can be explained by the intense radiation which occurs in much shorter lengths than in an amorphous material and which takes place, mainly, in the first mm of the crystal. Such solution could be interesting from the point of view of heating, as most of the power is deposited in the second part of the target (amorphous).
- The behaviour of crystals submitted to intense incident beams is a relevant problem. The heating affects the field levels in the crystals but do not avoid the radiation process. This is confirmed by theoretical and experimental investigations. In the specific conditions associated with a crystal positron source such effects have been estimated. The first analysis of the radiation damages, for the crystal submitted to the SLC beam up to June 1996 shows promising results.

• Concerning the foreseen experiment, let us recall that the goniometer has at least two crystal locations and that a comparison between two targets can take place rapidly.

In conclusion, the use of crystals in positron sources offers a large set of possibilities. Their main characteristics have been simulated, however an experimental test constitutes the best way to get definite data on this kind of source before recommending them for use in a linear collider.

Acknowledgments

We are grateful to Professor Jacques Lefrançois and Dr. François Richard for continuous support and stimulating discussions and to Dr. François Couchot for his interest and for many valuable remarks. We greatly appreciated the significant contribution of Manoel Dialinas and Guy Le Meur in the thermic simulations with finite elements

programs. We also thank the other colleagues of the collaboration, from BINP-Novosibirsk, IPN-Lyon and MPI-Stuttgart for punctual contributions in this report.

References

[1] X. Artru *et al.* Positron source using channeling in a tungsten crystal. *NIM A* **344** (1994) 443. See also contributions of R. Chehab and A. Jejcic in "Proceedings of the workshop on new kinds of positron sources for linear colliders", SLAC, March 4–7, 1997, SLAC-R-502.
[2] International Linear Collider Technical Review Committee Report – 1995, SLAC-R-95-471.
[3] V.N. Baier *et al.* Experimental test of a positron source using channeling and dedicated to future linear colliders (presentation at the LAL Scientific Council, Seillac June 96).
[4] X. Artru *et al.* Axial channeling of relativistic electrons in crystals as a source for positron production. *NIM B* **119** (1996) 246.
[5] V.N. Baier *et al.* Electromagnetic showers in crystals at GeV energies. *NIM B* **103** (1995) 147.
[6] R. Helm, Adiabatic approximation for dynamics of a particle in the field of a tapered solenoïd, SLAC-4, 1962.
[7] S. Ecklund, Positron target material tests, SLAC-CN-128, 1981.
[8] M. Dialinas, Utilisation du code aux éléments finis SYSTUS pour la simulation de l'échauffement d'une cible de tungstène sous l'impact d'un faisceau intense d'électrons, Note à paraître – November 96, Orsay.
[9] G. Le Meur, Thermic simulations with the finite elements program PRIAM/PROMETHEE developped at LAL, November 96, Orsay.
[10] V.N. Baier *et al.* Radiation yield of high-energy electrons in thick crystals. *Phys. Stat. Sol. (b)* **133** (1986) 583.
[11] D. Gemmel, *Review of Modern Physics* **46**(2) (1974) 129.
[12] S. Ecklund, Positrons for linear colliders, SLAC-PUB 4484, (Nov. 87).
[13] A. Kulikov (SLAC), Private communication.
[14] S. Baker *et al. Nucl. Instr. and Methods B* **90** (1994) 119.